

THERMO-XRD-ANALYSIS OF Co-, Ni- AND Cu-MONTMORILLONITE TREATED WITH ANIONIC ALIZARINATE

Curve-fitting

M. Epstein^{1,2}, I. Lapidés² and S. Yariv^{2*}

¹Tel-Hai Technological College, Upper Galilee 12210, Israel

²Department of Inorganic and Analytical Chemistry, The Hebrew University of Jerusalem, Jerusalem 91904, Israel

Co- and Ni-montmorillonites adsorb in aqueous suspensions up to 13 mmol alizarinate per 100 g clay, onto the broken-bonds whereas Cu-clay adsorbs up to 25 mmol dye per 100 g clay into the interlayer space. Unloaded Co-, Ni- and Cu-clays and samples loaded with increasing amounts of alizarinate, were gradually heated in air to 360°C and analyzed by X-ray diffraction. All diffractograms were curve-fitted. Fitted diffractograms of non-heated samples, showed two peak components labeled C and D, at ≈ 1.22 and ≈ 1.32 nm, characterizing tactoids with mono- and non-complete bilayers of water, respectively. After heating at 120°C component D decreased or disappeared and two new components A and B appeared at ≈ 0.99 and ≈ 1.08 nm, representing collapsed tactoids and tactoids with interlamellar oxy-cations, respectively. At 250°C C and D decreased or disappeared but A and B appeared in all fitted diffractograms. Co- and Ni-clay after heating at 360°C did not show C and D. Components A and B proved that these clays collapsed indicating that initially there was no alizarinate in the interlayers. At 360°C C and D persisted in the fitted-diffractograms of Cu-clay, representing tactoids with interlamellar charcoal formed from the partial oxidation of adsorbed dye initially located in the interlayers.

Keywords: alizarin, Co-montmorillonite, Cu-montmorillonite, curve-fitting, Ni-montmorillonite, thermo-XRD-analysis

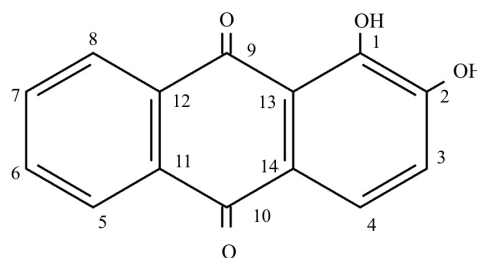
Introduction

Organic anions are adsorbed by clay minerals either onto positive-charged broken-bonds at the external surface of the clay crystals [1] or into the interlayer space, by forming positively charged coordination species with metallic cations [2, 3]. Adsorption on the external surface may change the colloidal behavior of the clay [4], whereas adsorption into the interlayer space may change the chemical and physical properties of the adsorbed species [5, 6]. Large organic anions are water structure breakers and as a result of their presence in the interlayer, the properties of this space are also changed [7].

The present paper is an enlargement of a previous [8] thermo-XRD analysis of the complexes of Co-, Ni- and Cu-montmorillonite with alizarinate, a deprotonated anionic variety of alizarin (Scheme 1). These transition metal cations form stable six-member chelate ring metal-ligand *d*-complexes with alizarinate through the deprotonated 1-hydroxyl oxygen and the adjacent carbonyl oxygen [9–15]. When these complexes were precipitated from aqueous-ethanol solutions, the metal:ligand molar ratio was 1:2 [15]. In our previous paper [8], we showed that the adsorbed alizarinate intercalated the interlayer space of Cu-montmorillonite but not of Co- or Ni-montmorillonite. This was determined

by thermo-XRD analysis. The clay samples were heated to 120, 250 and 360°C and diffracted by X-ray. A temperature of 360°C is above the dehydration temperature of these three clays. As a result of dehydration, the unloaded clays were collapsed.

In the presence of organic matter, oxidation occurs at above 250°C [16–18]. If the organic matter is present in considerable amounts, the oxygen in air is not sufficient for its complete oxidation; H₂O and charcoal are obtained by heating up to 360°C, the latter being identified by the black coloration of the clay [19]. If the organic matter has been adsorbed into the interlayer space, charcoal is formed inside this interlayer, preventing the thermal collapse of the clay [20]. At higher temperatures this charcoal is further oxi-



Scheme 1 Alizarin (1,2-dihydroxyanthraquinone)

* Author for correspondence: yarivs@vms.huji.ac.il

dized in two steps to CO₂ [21]. Cebulak *et al.* observed a similar multistep oxidation during the thermal analysis of natural resins in the presence of oxygen [22].

If the powdered clay mixtures used for the X-ray diffraction are homogeneous, than sharp X-ray peaks are recorded with integral series of high order reflections. But it is not very often that the clay mixtures are homogeneous. If there are tactoids with different basal spacings, the X-ray diffraction peak is broad with no integral series of high order reflections. This broad peak is composed of several components, each describing the basal spacing of several similar tactoids and the recorded peak is an average of these components. Sometimes two or more separate peaks are recorded but more often a peak with shoulders is recorded. If the relative amount of tactoids with the same basal-spacing is small, the information about their spacing may be lost in non-fitted diffractograms. Our previous preliminary study [8] was carried out without fitting of the diffractograms. The conclusions on the location of the adsorbed dye were therefore based on data obtained for samples with maximum adsorption.

In this paper, we present the results of curve fitting of the XRD diffractograms that were superficially discussed in our previous study. In spite of the fact that curve-fitting analysis has been widely used in the IR study of clays [23], and recently also in electronic spectroscopy studies of organo-clays [6, 24], it has not been used in thermo-XRD-analysis of organo-clay complexes. It is, therefore, necessary to examine comprehensively the physical meaning of each component of the broad peak.

Basal spacings recorded before the dehydration stage, characterize the hydrated state of the interlayer. They are usually above 1.2 nm, due to the presence of one or more water layers. Water monolayers give a basal spacing of 1.2–1.25 nm [25]. Water bilayers in Mg-smectites, where there are 12 water molecules per each cation, give a spacing of 1.52 nm (water of zone A_0 , according to the labeling of Yariv [26]). Non-complete water bilayers give lower spacings. In partial dehydrated vermiculite, where metallic cations are hexagonally coordinated by water molecules (water of zone A_m), give a basal spacing of 1.4 nm. In this case the water molecules are highly polarized forming strong hydrogen bonds with atoms of the clay-oxygen plane. Strong hydrogen bonds are also formed between non-structured water (water of zone B_{om}) and the oxygen plane. An alternative explanation to basal spacing is based on interstratification of hydrated smectites. According to Moore and Hower [27] at a relative humidity from 12 to 65% there is a regular interstratification of one water layer and anhydrous interlayer. According to Cases *et al.* [28], Na-montmorillonite is an interstratified layer

system of 0–3 water layer hydrates, and the degree of hydration increases with the relative humidity.

After a complete dehydration of unloaded or organo-montmorillonites with no organic material in the interlayer space, the spacing drops to 0.97–1.00 nm, due to the collapse of the interlayer. In the presence of intercalated organic matter, in spite of the dehydration, a spacing of above 1.15 nm is obtained after thermal treatment at about 300°C, due to the formation of charcoal in the interlayer [20].

In order to adsorb alizarin in its monovalent anionic form, the clay was treated with alkaline solutions (pH=8.7) of alizarin. At this pH, alizarin occurs mostly as a monoanion. As shown in our previous paper [6], depending on the exchangeable cation and on the dye/clay ratio in the suspension, alizarinate is adsorbed by montmorillonite in different amounts. The maximum amounts adsorbed by Na-, Co-, Ni-, Cu- and Al-montmorillonite were 4, 13, 13, 25 and 25 mmol/100 g, respectively. However, only part of the dye in the suspension is adsorbed by the clay, and there is an equilibrium between adsorbed and free non-adsorbed alizarinate in the supernatant.

Experimental

Materials

Alizarin was supplied by Sigma and was used as received. According to specification tests of the manufacturer there was 1% sulfated ash. Thin-layer chromatography and pH transition showed purity corresponds to standards. Aqueous NaH-alizarinate stock solution was prepared from neat alizarin dissolved in 0.001 M NaOH solution with a final pH of 9.2±0.2. A 5·10⁻⁴ M alizarinate solution was used as a stock solution.

Na-montmorillonite (Wyoming bentonite) was supplied by Wards' Natural Science Establishment, Inc. The clay was ground and sieved to 80 mesh. It was purified from quartz and other non-clay minerals by separation of the sedimented non-colloidal material from a 2% aqueous suspension. Na-montmorillonite was transformed to Co- Ni- and Cu-montmorillonite by suspending 2 g of the purified Na-clay for 24 h in 40 mL of 0.1 M of the nitrate salts. The monoionic clays were washed four times in 200 mL of distilled water and separated by centrifugation (4000 rpm for 15 min). Suspensions of 1.0% monoionic clay were used as stock solutions.

Methods

Alizarinate loaded samples of Co- Ni- and Cu-montmorillonite for XRD were prepared as follows: The clay suspensions were diluted by distilled water to the

Table 1 Characteristic features of curve-fitted X-ray diffractograms of unloaded Co-montmorillonite and of Co-montmorillonite loaded with increasing amounts of alizarinate before and after thermal treatments at 120, 250 and 360°C (peak component maxima, in nm, relative peak areas, in % of total peak area, and widths at half height, in °2θ). All samples were diffracted at room temperature

Loading	Adsorbed dye/mmol/100 g	Temp/°C	Component A		Component B		Component C		Component D	
			maximum/nm	Relative area/%	maximum/nm	Relative area/%	maximum/nm	Relative area/%	maximum/nm	Relative area/%
0	0	RT					1.19	16	1.33	84
		120					1.15	85	1.30	15
		250	1.01	40	1.06	46	1.24	14		
		360	0.99	75	1.06	25				
5	4	RT					1.21	61	1.27	39
		120			1.10	75	1.22	25		
		250	1.01	26	1.06	58	1.19	16		
		360	0.99	72	1.08	28				
10	8	RT					1.22	72	1.28	28
		120			1.08	71	1.20	29		
		250	1.01	38	1.08	41	1.19	21		
		360	0.98	68	1.06	32				
20	13	RT					1.22	72	1.27	28
		120	1.00	26	1.05	49	1.20	25		
		250	0.99	56	1.06	28	1.24	16		
		360	0.96	76	1.06	24				
50	13	RT					1.22	73	1.36	27
		120	0.98	14	1.05	29	1.16	57		
		250	0.97	48	1.06	31	1.23	21		
		360	0.96	66	1.06	34				

Table 2 Characteristic features of curve-fitted X-ray diffractograms of unloaded Ni-montmorillonite and of Ni-montmorillonite loaded with increasing amounts of alizarinate before and after thermal treatments at 120, 250 and 360°C (peak component maxima, in nm, relative peak areas, in % of total peak area, and widths at half height, in °2θ). All samples were diffracted at room temperature

Loading	Adsorbed dye/mmole/100 g	Temp/°C	Component A		Component B		Component C		Component D		Relative area/%	Width/2θ
			maximum/nm	Relative area/%	maximum/nm	Relative area/%	maximum/nm	Relative area/%	maximum/nm	Relative area/%		
0	0	RT					1.23	40	1.0	1.34	60	1.6
		120					1.15	98	1.7	1.55	2	1.5
		250	1.00	18	0.7	1.07	42	1.5	2.5			
		360	0.98	70	0.8	1.06	30	2.3				
5	2	RT					1.22	57	0.8	1.32	43	1.9
		120	1.01	11	0.6	1.06	38	1.3	1.4	1.33	11	2.0
		250	1.01	34	0.9	1.09	32	1.3	1.4	1.34	17	2.9
		360	0.99	65	0.6	1.07	35	1.7				
10	3	RT					1.21	75	0.9	1.25	25	2.2
		120					1.18	59	1.3	1.37	13	3.2
		250	0.99	46	0.7	1.06	31	1.2	2.0	1.35	5	1.4
		360	0.98	62	0.6	1.06	28	1.5				
20	5	RT					1.21	79	0.9	1.32	21	2.9
		120					1.14	51	1.4	1.35	20	2.6
		250	0.97	56	0.6	1.05	28	1.2	0.5	1.38	12	1.9
		360	0.97	67	0.6	1.05	33	1.5				
50	13	RT					1.23	73	0.8	1.36	27	1.8
		120					1.19	75	1.3	1.48	12	2.2
		250	0.98	40	0.7	1.05	20	0.7	1.9			
		360	0.98	73	0.77	1.09	27	1.6				

Table 3 Characteristic features of curve-fitted X-ray diffractograms of unloaded Cu-montmorillonite and of Cu-montmorillonite loaded with increasing amounts of alizarinate before and after thermal treatments at 120, 250 and 360°C (peak component maxima, in nm, relative peak areas, in % of total peak area, and widths at half height, in °2θ). All samples were diffracted at room temperature

Loading	Adsorbed dye/mmol/100 g	Temp/°C	Component A maximum/nm	Relative area/%	Width/2θ	Component B maximum/nm	Relative area/%	Width/2θ	Component C maximum/nm	Relative area/%	Width/2θ	Component D maximum/nm	Relative area/%	Width/2θ
0	0	RT							1.22	69	0.6	1.32	31	2.06
		120							1.16	87	1.1	1.42	13	3.8
		250	1.01	83	0.7	1.13	17	2.0						
		360	0.99	81	0.6	1.08	19	1.6						
5	5	RT							1.23	66	0.5	1.31	34	1.6
		120							1.18	97	1.1	1.50	3	1.2
		250	1.01	31	0.8	1.05	44	0.8	1.15	25	1.4			
		360	0.99	54	0.6	1.05	30	0.8	1.15	16	1.4			
10	8	RT							1.23	72	0.4	1.29	28	1.4
		120	nd											
		250				1.07	23	1.1	1.20	72	0.9	1.46	5	1.5
		360	0.99	38	0.6	1.07	44	1.0	1.23	18	2.0			
20	15	RT							1.24	75	0.4	1.30	25	1.2
		120				1.11	14	1.3	1.22	78	0.7	1.38	8	2.1
		250				1.08	10	1.1	1.22	80	0.7	1.37	10	2.4
		360	0.98	4	0.3	1.03	12	0.7	1.15	84	1.7			
50	21	RT							1.25	75	0.5	1.34	25	1.7
		120				1.12	10	1.1	1.23	71	0.7	1.33	19	1.6
		250				1.14	8	1.5	1.24	61	0.6	1.32	31	1.7
		360	0.99	4	0.4	1.07	5	0.4	1.19	84	1.2	1.30	7	1.3

required concentration and treated in an ultrasonic bath for 10 min before adding the alizarinate solution. The aqueous clay suspensions were loaded by the required amount of NaH-alizarinate (5, 10, 20, and 50 mmol alizarinate /100 g clay) by slowly dropping the dye aqueous solution into the suspension with vigorous shaking. The clay adsorbed only part of the added dye. The adsorbed amount in each case will be shown in the following Tables. The final volume of each suspension was 12 mL and its final clay concentration 0.1%. Suspensions were left for 48 h in measuring cylindrical tubes. After the sedimentation of the clay to a volume of about 1.0 mL, the upper 11.0 mL water, which contained most of the excess non-adsorbed dye, was decanted. The 1.0 mL concentrated clay suspensions were air dried on microscope glasses giving oriented films.

The XRD measurements of the dried samples were made at room temperature and in air atmosphere. Samples were diffracted before any thermal treatment and after heating at 120, 250 and 360°C during three hours at each temperature. XRD diffractograms were recorded by using a Philips Automatic Diffractometer (PW 1710) with a Cu tube anode.

Curve-fitting of the diffractograms was made by using Phillips' APD software.

Results and discussion

Tactoids or oriented aggregates are clusters of parallel layers held by face-to-face interactions (FF associations). According to Bragg's Law, particles obtained from FF associations of similar layers, and have similar interlayer spaces, may diffract X-rays. Originally the term 'tactoids' was used to describe particles in suspensions and colloid solutions. Here it is used for solid particles capable to diffract X-rays in powder mixtures.

Figures 1A, B, C and D presents the curve-fitted XRD diffractograms of alizarinate-treated Co-montmorillonite unheated and heated at 120, 250 and 360°C, respectively. Similar curves were obtained for Ni- and Cu-montmorillonite loaded with different amounts of alizarinate. Features of all fitted curves, e.g. peak components, their relative areas (in percents from the total area) and widths (in 2θ) in the diffractograms of Co-, Ni- and Cu-montmorillonite are gathered in Tables 1, 2 and 3, respectively. The effects of the amount of adsorbed alizarinate and of the thermal treatments on the locations of the maxima and relative areas of the peak components in the diffractograms of the different clays are discussed hereby.

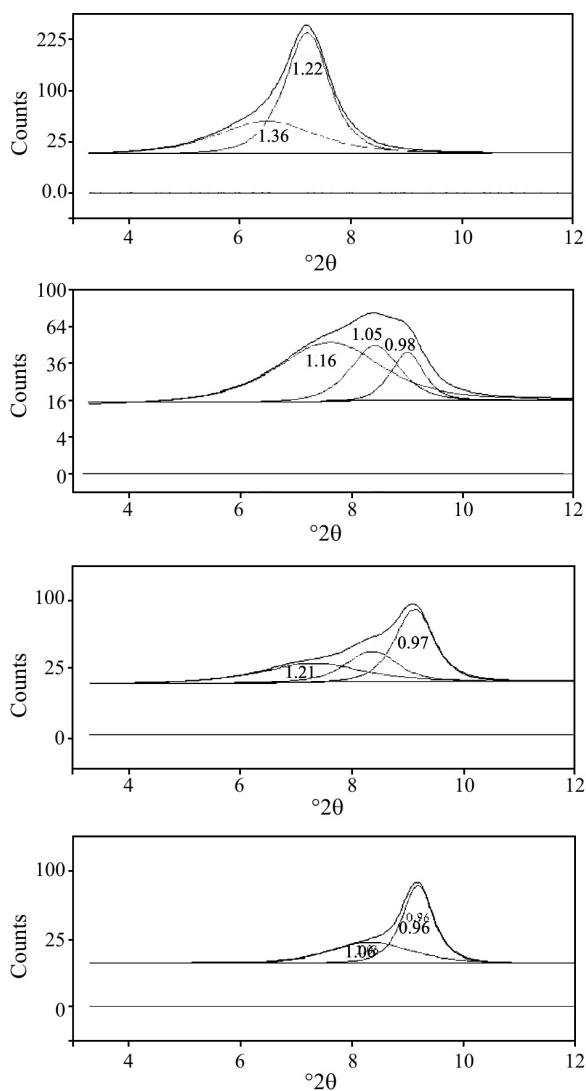


Fig. 1 Curve-fitted XRD diffractograms of Co-montmorillonite treated with alizarinate (50 mmol/100 g clay) at room temperature (A) and after thermal treatments at 120, 250 and 360°C (B, C and D, respectively)

Curve-fitted diffractograms of unloaded and of alizarinate-loaded montmorillonite before the thermal treatment

Curve-fitted diffractograms of unloaded and loaded Cu-montmorillonite before thermal treatment are presented in Fig. 2 (A and B respectively). Similar curves were obtained for Co- and Ni-montmorillonite. Curve-fitted diffractograms of non-heated clays showed two peak components, labeled C and D, with maxima at 1.22 ± 0.03 and 1.32 ± 0.05 nm, which may characterize tactoids with interlamellar planar water monolayers and non-complete water bilayers (or water in excess to monolayers), respectively.

From the table it is obvious, that with Co- and Ni-clay the relative area of peak component D sharply

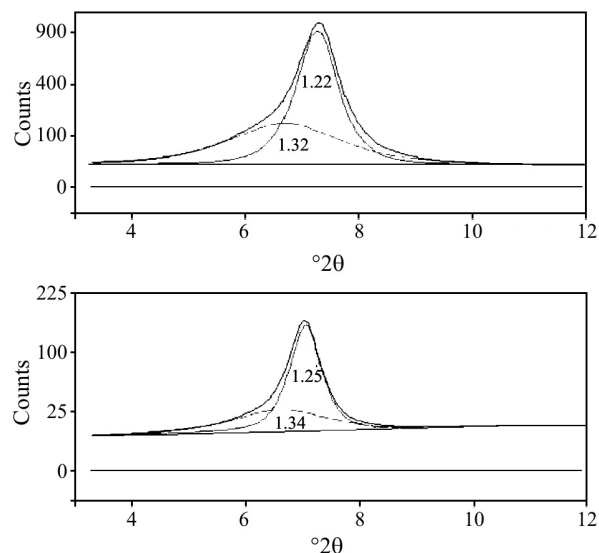


Fig. 2 Curve-fitted XRD diffractograms of Cu-montmorillonite before thermal treatment - unloaded and loaded with 50 mmol alizarinate /100 g clay (A and B, respectively)

decreased with increasing amount of alizarinate up to adsorption of 8 and 3 mmol per 100 g clay, respectively, whereas the area of peak component C increased. It can be explained due to the increasing hydrophobicity of the clay with the adsorption of organic matter [29]. With Cu-montmorillonite, the relative area of component D did not change with the addition of alizarinate ($30 \pm 5\%$ in all the diffractograms). The difference in behavior between Ni- and Co-montmorillonite on one hand and Cu-montmorillonite on the other should be noted. In the former clays, alizarinate is adsorbed onto the broken-bonds, namely, the organic matter which is located on the external surface of the clay, reduces the amount of water in the interlayer. In Cu-montmorillonite, the dye is adsorbed only into the interlayer space and not onto the broken-bonds surface but no effect on the hydrophilicity is observed.

Curve-fitted diffractograms of unloaded and of alizarinate-loaded montmorillonite after heating at 120°C

After heating the samples at 120°C, as a result of water evolution, the relative area of peak component D, which characterizes tactoids with interlamellar water in excess to a monolayer, decreased. In some cases it disappeared, indicating the dehydration of these tactoids and their transformation to the tactoids with interlamellar water monolayer. Some fitted diffractograms showed two new peak components, labeled A and B, at 0.99 ± 0.02 and 1.08 ± 0.02 nm, which are assumed to be associated with the clay dehydration. According to the location of its maximum, peak

component A should be attributed to collapsed interlayers, indicating the presence of tactoids with total dehydration and with no organic matter in this space.

Peak component B appeared with all alizarinate-loaded Co- and Ni-clays, but only with two of the loaded Cu-clay. The location of the maximum of this component is problematic. It is too high to account for collapsed interlayers and too short for swollen interlayers with intercalated water monolayers, yet it appeared in the fitted diffractograms of most alizarinate-loaded samples heated at 120°C and also in those of unloaded and loaded samples, which were heated at higher temperatures. According to MacEwan and Wilson [30], smectites containing large exchangeable cations, which are not able to penetrate completely into the hexagonal holes, in thermal collapse may give rise to basal spacings higher than 1.02 nm. A possible explanation is based upon formation of oxy- or hydroxy-cations in the interlayer space, as a result of hydrolysis of hydrated exchangeable metallic cations [31], or as a result of migration of water protons towards incompletely neutralized OH groups coordinated to Mg or Al in the octahedral sheet [32]. Hydrolysis becomes more significant with the thermal dehydration of the clay. It is supposed that component B characterizes tactoids with interlamellar oxy-cations that prevent a complete collapse. The nature of this component requires further study.

In the fitted diffractograms of unloaded Co- Ni- and Cu-montmorillonite (Tables 1–3), the relative areas of component D sharply decreased, from 84, 60 and 31% before the thermal treatment to 15, 2 and 13%, respectively, after heating at 120°C, and at the same time the relative areas of component C, which represents tactoids with water monolayers, increased. In the fitted diffractograms of alizarinate-loaded Co-clay samples, component D did not appear after the thermal treatment due to the escape of excess water. With alizarinate-loaded Ni-montmorillonite component D decreased in the fitted diffractograms of all samples after thermal treatment at 120°C, but unlike with Co-clay, it did not disappear. Ni-montmorillonite under similar loading treatments adsorbs alizarinate in smaller amounts (about 40%) than the Co-clay. Only with a loading of 50 mmol per 100 g the adsorbed amounts were similar in both monoionic clays. When the adsorbed amount of dye is lower, the hydrophobicity of the clay is expected to be weaker, and consequently, with Ni-clay component D still appeared at 120°C. With both samples the relative area of component C decreased significantly and broadened, becoming 2–3 times wider than before the thermal treatment. The widening of this component indicates that after the thermal treatment the tactoids attributed to component C became very inhomogeneous.

The disappearance or decrease of components D and C as a result of the thermal treatment, were accompanied by the appearance of two new components A and B. Peak component A appeared only with one sample of Co and one of Ni indicating that at 120°C collapse is not regular. Component B appeared with all alizarinate-treated samples, and its relative area decreased with the increasing amount of adsorbed dye.

In the fitted diffractograms of alizarinate-loaded Cu-montmorillonite (Table 3), like in those of Ni-clay, component D decreased with heating the clay to 120°C. The relative area of component C increased with low dye loadings or remained constant with the higher dye loadings. Since in Cu-montmorillonite alizarinate formed with copper a *d*-coordination complex inside the interlayer space, the excess water that forms component D and part of the water that forms component C evolved during the heating, but organic matter remained in the interlayer space. In this clay sample, in addition to tactoids with water monolayers, component C also represents tactoids with organic monolayers in the interlayer space, and therefore its relative area should not decrease although other peak components appear. This is also the reason why component D, that also represents tactoids with interlamellar water or organic molecules, did not disappear despite the hydrophobic character of the alizarinate-loaded Cu-clay. When these Cu samples were heated the width of component C almost did not change. It appears that the presence of interlamellar organic matter kept the tactoids from becoming inhomogeneous.

Curve-fitted diffractograms of unloaded and of alizarinate-loaded montmorillonite after heating at 250°C

Heating the clay samples at 250°C resulted in further dehydration, shown by the decrease in the relative areas of components C and D and the increase in the relative areas of components A and B in the fitted diffractograms. Components C and D disappeared from the diffractogram of unloaded Cu-montmorillonite, indicating that this clay lost its interlayer water at 250°C. Component C did not disappear from the diffractograms of unloaded Co- and Ni-montmorillonite, indicating that water was not completely evolved from these clays at 250°C.

All diffractograms of Co-montmorillonite showed components A and B but did not show component D (Table 1). The relative area of component C decreased and its width increased significantly due to the evolution of water. The broadening indicates that the thermal treatment at 250°C resulted in inhomogeneity of the remaining hydrated tactoids.

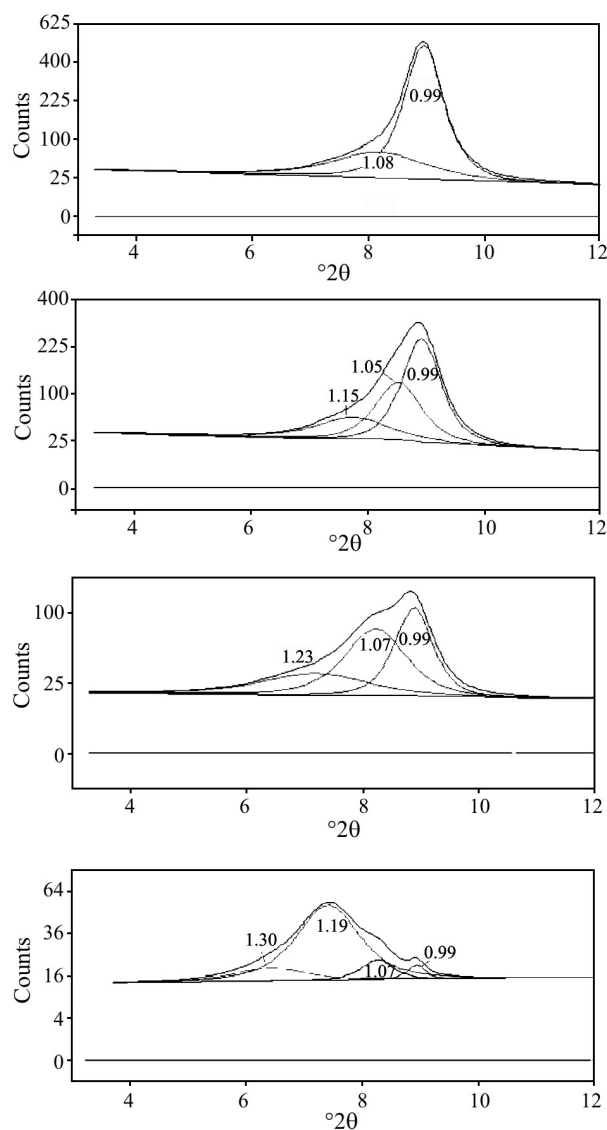


Fig. 3 Curve-fitted XRD diffractograms of Cu-montmorillonite, containing 0, 5, 8 and 21 mmol alizarinate 100 g clay, heated at 360°C (A, B, C and D, respectively)

In the fitted diffractograms of Ni-montmorillonite component D persisted in the alizarinate-loaded samples (except for the most highly loaded sample), suggesting their weaker hydrophobicity (Table 2). Only when the adsorbed alizarinate was 13 mmol per 100 g clay component D was not observed. The relative area of component C decreased in all the fitted diffractograms compared with those of the samples heated at 120°C. Component A appeared with all samples due to the dehydration and collapse.

In Cu-montmorillonite component A did not appear with the highly-loaded clays, due to the presence of organic matter in the interlayer space, which prevented the collapse (Table 3). Components C and D which did not appear in the unloaded clay, due to its complete dehydration, appeared in the loaded clay

diffraction patterns due to the presence of interlamellar organic matter. Because of the absence of water, the maxima of these components can give some information on the arrangement of alizarinate in the interlayers in the different types of the tactoids. The van der Waals diameter of carbon is about 0.34 nm and consequently component C with a maximum at 1.15–1.24 nm, is attributed to tactoids with monolayers of alizarinate anions lying between the clay layers, the aromatic rings being parallel to the oxygen planes, with keying of some of the atoms into the hexagonal holes of the clay-oxygen planes. Component D with a maximum at 1.32–1.46 nm, is attributed to tactoids with alizarinate anions slightly tilted between the layers relative to the oxygen planes. Component D appeared only with amounts of adsorbed alizarinate higher than 8 mmol per 100 g clay. The spacing of these tactoids decreased with increasing amounts of adsorbed dye, suggesting that the tilting angle relative to the clay-oxygen plane decreased with increasing amounts of adsorbed dye.

Curve-fitted diffractograms of unloaded and of alizarinate-loaded montmorillonite after heating at 360°C

Only components A and B but not C and D appeared in the fitted diffractograms of unloaded and alizarinate-loaded Co- and Ni-montmorillonites heated at 360°C, due to their dehydration and collapse (Tables 1 and 2). Their collapse at 360°C proves that the initially adsorbed alizarinate was not located in the interlayer space. Ratios between relative areas of components A and B in the fitted diffractograms of Co- and Ni-clays, whether they were loaded or not, were 2.5 ± 0.5 and 2.1 ± 0.5 , respectively. It should be noted that these ratios did not depend on the adsorbed alizarinate.

Curve-fitted diffractograms of Cu-montmorillonite, unloaded and loaded with varying amounts of alizarinate and heated at 360°C are presented in Fig. 3 (A, B, C and D for samples containing 0, 5, 8 and 21 mmol per 100 g, respectively). The relative area of component A sharply decreased with increasing amount of adsorbed alizarinate, from 81% with untreated clay to 4% with clay samples containing 15–21 mmol dye per 100 g clay, indicating that in the latter most of the clay did not collapse (Table 3). Components C and D characterize tactoids with two kinds of charcoal in the interlayer space, the former with a basal spacing of 1.16–1.19 nm and the latter with a spacing of 1.30 nm. Component C appeared with all the loaded samples and its relative area increased with the amount of adsorbed dye up to a maximum of 84% with adsorption of 21 mmol per 100 g clay. Component D appeared only with the highest loading. Since at

360°C the clay dehydration was complete, the appearance of component C indicated the presence of tactoids with monolayer charcoal formed between the lamellae from the partial oxidation of the adsorbed organic dye initially located in the interlayer space. Since the van der Waals diameter of carbon is 0.34 nm and the collapsed clay has a spacing of 0.97 nm, a spacing of 1.15–1.19 is too short for a monolayer charcoal to be lying in the interlayer space. Previously, in the study of organo-clays, for a similar spacing, it was suggested that carbon atoms were keying into the hexagonal holes of the clay-oxygen plane [33]. The appearance of component D indicates the presence of tactoids with monolayer charcoal with no penetration into the hexagonal holes. The appearance of components C and D proves that in Cu-montmorillonite, in contrast to Co- and Ni-montmorillonite, alizarinate, which is the charcoal precursor, initially intercalated into the interlayer space.

Conclusions

Curve-fitting of the XRD diffractograms recorded after heating unloaded and alizarinate-loaded montmorillonites at different temperatures showed a development of peak components, change in their characteristic features and disappearance as a result of the thermal treatments. Four peak components were identified which are supposed to characterize tactoids with collapsed, partly collapsed and two types of swollen interlayers. In order to establish whether the adsorbed organic species was located in the interlayer space of the clay, it was necessary to heat the samples to 360°C, a temperature at which the interlamellar organic species forms charcoal. Alizarinate-loaded Cu-montmorillonite showed the formation of charcoal in its interlayer space but Alizarinate-loaded Co- and Ni-clays did not show it, suggesting that in the former, the charcoal precursor alizarinate was adsorbed into the interlayer but in the latter it was adsorbed onto the external surface.

In order to find out the arrangement of the organic species inside the interlayer space, it was necessary to heat the samples to 250°C, a temperature above the dehydration stage of the Cu-clay. Two types of alizarin-Cu-montmorillonite complexes were identified. In one type alizarinate anions were lying between the layers, the aromatic rings being parallel to the oxygen planes and in the second type, alizarinate anions were slightly tilted between the layers relative to the clay-oxygen planes.

At room temperature relatively intense diffractions were recorded from tactoids with water in the interlayers, with basal spacings very similar to those of the tactoids containing the alizarinate species. Af-

ter dehydration, due to their high quantity, diffraction of collapsed tactoids may conceal the diffractions of the relatively small amounts of tactoids containing the organic dye, which may be present in the interlayer space. Curve-fitting calculation of the diffractograms enables the identification of the peak components resulting from the diffraction of tactoids, which contained the organic species in their interlayer space.

References

- 1 S. Yariv and K. H. Michaelian, *Schrieffenr. Angew. Geowiss.*, 1 (1997) 181.
- 2 S. Yariv and W. Bodenheimer, *Israel J. Chem.*, 2 (1964) 197.
- 3 S. Yariv, in 'Organo-clay complexes and interactions' (S. Yariv and H. Cross, Eds) Marcel Dekker, New York, 2002, p. 39.
- 4 H. van Olphen, 'Clay colloid chemistry' Interscience, New York, 1963, p. 160.
- 5 S. Yariv, in 'Organo-clay complexes and interactions' (S. Yariv and H. Cross, Eds) Marcel Dekker, New York, 2002, p. 463.
- 6 M. Epstein and S. Yariv, *J. Colloid Interface Sci.*, 263 (2003) 377.
- 7 L. Heller-Kallai and S. Yariv, *J. Colloid Interface Sci.*, 79 (1981) 479.
- 8 M. Epstein, I. Lapidés and S. Yariv, *Colloid Polym. Sci.*, (2004) in press.
- 9 S. Das, A. Saha and P. C. Mandal, *Talanta*, 43 (1996) 95.
- 10 S. Das, A. Bhattacharya, P. C. Mandal, M. C. Rath and T. Mukherjee, *Radiat. Phys. Chem.*, 65 (2000) 93.
- 11 F. Feigl, 'Chemistry of specific, selective and sensitive reactions', Academic Press, New York, 1949.
- 12 M. Lalia-Kantouri and M. Bakola-Christianopoulou, *Polyhedron*, 3 (1984) 729.
- 13 M. Lalia-Kantouri and M. Bakola-Christianopoulou, *Thermochim. Acta*, 104 (1986) 39.
- 14 L. J. Larson and J. L. Zink, *Inorg. Chim. Acta*, 169 (1990) 71.
- 15 M. N. Bakola-Christianopoulou, *Polyhedron*, 3 (1984) 729.
- 16 S. Yariv, *Appl. Clay Sci.*, 24 (2004) 225.
- 17 A. Langier-Kuzniarowa, in 'Organo Clay Complexes and Interactions' (S. Yariv and H. Cross, Eds) Marcel Dekker, Inc., New York, 2002, p. 273.
- 18 S. Yariv, in 'Natural and Laboratory Simulated Thermal Geochemical Processes', (R. Ikan, Ed.), Kluwer Academic Press, 2003, p. 253.
- 19 W. Bodenheimer, L. Heller and S. Yariv, *Clay Minerals*, 6 (1966) 167.
- 20 Z. Yermiyahu, I. Lapidés and S. Yariv, *J. Therm. Anal. Cal.*, 69 (2002) 317.
- 21 Z. Yermiyahu, A. Landau, A. Zaban, I. Lapidés and S. Yariv, *J. Therm. Anal. Cal.*, 72 (2003) 431.
- 22 S. Cebulak, A. Matuszewska and A. Langier-Kuzniarowa, *J. Therm. Anal. Cal.*, 71 (2003) 905.
- 23 K. H. Michaelian, W. I. Friesen, S. Yariv and A. Nasser, *Can. J. Chem.*, 69 (1991) 1786.
- 24 Z. Yermiyahu, I. Lapidés and S. Yariv, *Clay Minerals*, 38 (2003) 483.
- 25 F. Kraehenbuehl, H. F. Stoeckli, F. Brunner, G. Kahr and M. Mueller-Vonmoos, *Clay Minerals*, 22 (1987) 1.
- 26 S. Yariv, in 'Modern Approaches to Wettability: Theory and Applications' (M. E. Schrader and G. Loeb, Eds), Plenum Press, New York, 1992, p. 279.
- 27 D. M. Moore and J. Hower, *X-ray Diffraction and the Identification and Analysis of Clay Minerals*, Oxford University Press, Oxford, 1986.
- 28 J. Cases, I. Berend, G. Besson, M. François, J. P. Uriot, F. Thomas and J. E. Poirier, *Langmuir*, 11 (1992) 2734.
- 29 R. F. Giese and C. J. van Oss, in *Organo Clay Complexes and Interactions*, (S. Yariv and H. Cross, Eds) Marcel Dekker, Inc., New York, 2002, p. 175.
- 30 D. M. C. MacEwan and M. J. Wilson, in 'Crystal Structure of Clay Minerals and their X-ray Identification', Monograph 5, (G. W. Brindley and G. Brown, Eds) Mineralogical Society, London, 1980, p. 197.
- 31 C. E. Marshall, *The Colloid Chemistry of the Silicate Minerals*. Academic Press, Inc., New York, 1949, p. 121.
- 32 J. D. Russell and A. R. Fraser, *Clays Clay Miner.*, 19 (1971) 55.
- 33 W. Bodenheimer, L. Heller, B. Kirson and S. Yariv, *Clay Minerals*, 5 (1962) 145.

DOI: 10.1007/s10973-005-6856-8